π-equivalent representation [5] of the new Y'-parameters as [6]

$$C_{ob} = \frac{\mathrm{Im}(-y'_{12})}{\omega} \tag{11}$$

$$C_{be} = \frac{1}{\omega}\mathrm{Im}(y'_{11} + y'_{12}) \tag{12}$$

$$g_m = |y'_{21} - y'_{12}|. \tag{13}$$

Finally, both $f_{c,\max}$ and $f_{p,\max}$ are calculated by inserting the elements values obtained from (9) to (13) into (5) and (8).

In Table I, both $f_{c,\max}$ and $f_{p,\max}$ are computed with $R_E = 100\ \Omega$ in the first two columns. The transistors are biased to $V_{CE} = 2.5$ V and $I_E = 3$ mA and packaged with low-cost plastic-mold types.[1] For comparison, the results obtained from S-parameters are also summarized in the last two columns $f_{\max\_S}$ and f_{osc_S}, respectively. As compared in Table I, $f_{p,\max}$ is in relatively good agreement with f_{osc_S}, but the estimated $f_{c,\max}$ needs some further improvements. The discrepancy between $f_{c,\max}$ and $f_{\max\_S}$ may be from the fact that the small-signal equivalent circuit [as in Fig. 4(a)] does not represent the measured S-parameters very well near the frequency $f_{\max}$. It is also shown in Table I that to apply this VCO circuit at 2 GHz, transistors with $f_{\max}$ higher than 4 GHz are required.

IV. Conclusion

For the presented VCO circuit, new formulas for estimating the maximum frequency of oscillation were developed. $f_{p,\max}$ shows the strong dependence on the emitter bias resistor in the region of small R_E, which greatly reduces the oscillation capability of the transistor itself. To prevent the degradation, the voltage drop across the emitter resistor should not be set so small. The formulas can be used as a practical guide in choosing the active devices for the presented VCO circuit.

The validity of the formula is verified by comparing the results with those obtained from replacing the transistors by the measured two-port S-parameters. The comparison shows that $f_{p,\max}$ computed from the unilateral equivalent circuit is in good agreement with that obtained from the S-parameters. For the given R_E, the $f_{p,\max}$ computation with an equivalent circuit is somewhat tedious compared with the direct S-parameter replacement. However, if done, one may find that the proper R_E does not significantly degrade the oscillation capability for the chosen device. In addition, it can be determined whether or not the chosen device is adequate for the presented structure at a given supply voltage.

References

[1] ETSI, "European digital cellular telecommunications system (phase 2); radio transmission and reception," GSM 05.05 (version 4.60), July 1993.

[2] Y. Fonda, "VCO techniques enable compact, high frequency mobile-com," *J. Electr. Eng.*, pp. 40–43, Dec. 1993.

[3] T. Nishimoto, "RF front end circuit components miniaturized using dielectric resonators for cellular portable telephones," *IEICE Trans.*, vol. E74, no. 6, pp. 1556–1562, June 1991.

[4] H. Fukui, *Low Noise Microwave Transistors & Amplifiers.* Piscataway, NJ: IEEE Press, 1981, pp. 68–86.

[5] W. H. Kim and H. E. Meadows, Jr., *Modern Network Analysis.* New York: Wiley, 1971, p. 222.

[6] K. W. Yeom *et al.*, "Frequency dependence of GaAs FET equivalent circuit elements extracted from the measured S-parameters," *Proc. IEEE*, vol. 76, pp. 843–845, July 1988.

[1] NEC Microwave Semiconductors, California Eastern Laboratory, Santa Clara, CA, 1994.

A New Approach to Nonlinear Analysis of Noise Behavior of Synchronized Oscillators and Analog-Frequency Dividers

J. C. Nallatamby, M. Prigent, J. C. Sarkissian, R. Quere, and J. Obregon

***Abstract*—An original theory of phase noise in synchronized oscillators is outlined through the phase-locked loop (PLL) approach. The phase-noise spectrum obtained first by the analytical PLL theory and then by the simulator developed in [1] have been compared with very good accuracy. This new approach permits the best understanding of noise conversion in synchronized devices.**

I. Introduction

The purpose of this paper is to outline a new approach to nonlinear analysis of noise behavior in potentially unstable circuits such as synchronized oscillators. The nonlinear noise theory for synchronized oscillators has been given by Schunemann [1]. Goedbloed and Vlaardingerbroek [2] calculated the transfer properties of the injection-locked oscillator. However, [1] and [2] give a good qualitative understanding of the noise behavior for the fundamentally synchronized oscillator only. A general expression for output FM noise calculation for subharmonic injection-locked oscillators was formulated in terms of injected phase noise, intrinsic noise of the free-running oscillator, and the injection locking range [3]. A complementary study with previous works and an original approach to evaluate noise in the injection-locking mechanism of an oscillator by the help of the analog phase-locked loop (PLL) theory will be discussed in detail. The phase-noise spectrum analytically obtained by the PLL approach is compared with the results of the nonlinear noise simulator developed in [4].

II. Noise in Synchronized Oscillator

Let us consider a Van Der Pol oscillator, shown in Fig. 1. A parallel resonant circuit (RLC) approximates the resonance structure. The voltage source $e(t)$ represents an intrinsic noise generator where the spectral density which varies with the law $\langle E(f)^2\rangle = (1e-9)/f$. $i_s(t)$ is the synchronizing current source. The active device is modeled by two elements with the Van Der Pol third-order polynomial characteristic

$$i(v) = b \cdot v + d \cdot v^3, \qquad \text{with } b = -0.02 \text{ and } d = 0.7\ q(v) = q_0 v. \tag{1}$$

This gives us a good understanding of the oscillator noise behavior because it contains the main nonlinearities of all transistor nonlinear models (MESFET, bipolar, heterojuction bipolar transistor (HBT), ...). We are now in a position to analytically calculate the contributions to the output noise spectrum due to both the intrinsic noise source $e(t)$ and to the injected current source $i_s(t)$.

A. Effects of Injected Noise

The noise sources considered here concern only the phase noise of the injection signal. It is possible to describe the noise of a synchronized oscillator via the analogy of phase-locking mechanism.

Manuscript received November 8, 1996; revised May 11, 1998.
The authors are with IRCOM-UMR CNRS 6615, 19100 Brive, France.
Publisher Item Identifier S 0018-9480(98)05501-X.

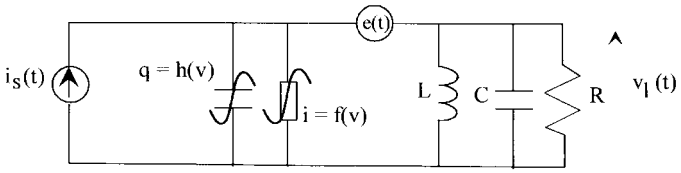

Fig. 1. Oscillator with Van Der Pol characteristic elements. $R = 68\ \Omega$, $L = 10.787$ pH, $C = 2.3475$ nF, for $f_0 = 10$ GHz.

Thus, this example will cover a theoretical study of the noise behavior of synchronized oscillator with the help of this analogy. The results will be compared with those provided by our simulator based on the conversion matrix approach [4]. The differential equation for the voltage $V_l(t)$ is

$$\frac{d^2V_l}{dt^2} + \frac{\omega_0^2}{Q_0}\cdot\frac{dV_l}{dt} + \omega_0^2\cdot V_l(t) + \frac{1}{C}\cdot\frac{di}{dt} = \frac{1}{C}\cdot\frac{di_s}{dt} \tag{2}$$

where $\omega_0 = 1/\sqrt{L\cdot C}$ is the resonant frequency and Q_0 is the quality factor of the parallel RLC. Due to the high Q_0, the output voltage $V_l(t)$ can be expressed as a sine-wave signal and the generator $i_s(t)$ can be written as

$$V_l(t) = \mathrm{Re}(\hat{V}_l(t)\cdot e^{j\cdot(\omega\cdot t+\varphi(t))})$$

and

$$i_s(t) = \mathrm{Re}(\hat{I}_s(t)\cdot e^{j\cdot(\omega\cdot t+\psi(t))}) \tag{3}$$

where $\hat{V}_l(t)$ describes the amplitude variation as a function of time and $\varphi(t)$ is the phase variation.

Substituting (3) into (2), we obtain

$$\begin{aligned}&\frac{d^2\hat{V}_l}{dt^2} + \left(\frac{\omega_0}{Q_0} + \frac{1}{C}\cdot\left(b + \frac{9}{4}\cdot d\cdot\hat{V}_l^2\right)\right)\cdot\frac{d\hat{V}_l}{dt}\\ &\quad + \left(\omega_0^2 - \left(\omega + \frac{d\varphi}{dt}\right)^2\right)\cdot\hat{V}_l\\ &\quad = -I_s\cdot\frac{\omega}{C}\cdot\sin(\psi-\varphi)\end{aligned} \tag{4}$$

$$\begin{aligned}&\frac{d^2\varphi}{dt^2} + \frac{2}{\hat{V}_l}\cdot\left(\omega + \frac{d\varphi}{dt}\right)\cdot\frac{d\hat{V}_l}{dt} + \left(\omega + \frac{d\varphi}{dt}\right)\\ &\quad\cdot\left(\frac{\omega_0}{Q_0}\cdot + \frac{1}{C}\cdot\left(b + \frac{3}{4}\cdot d\cdot\hat{V}_l^2\right)\right)\\ &\quad = \frac{I_s}{\hat{V}_l}\cdot\frac{\omega}{C}\cdot\cos(\psi-\varphi).\end{aligned} \tag{5}$$

By taking into account the free and synchronized regimes of the oscillator and the assumption of $d\varphi/dt \ll \omega$, (4) and (5) lead to

$$\frac{d\varphi}{dt} - \frac{I_s}{2\cdot C\cdot\hat{V}_l}\cdot\sin(\psi-\varphi) = \Delta\omega_0 \tag{6}$$

where $\Delta\omega_0 = \omega_0 - \omega$ is the offset frequency from free-running oscillation frequency. This equation is called an Adler's phase equation [4]. For the steady state ($d\varphi/dt = 0$) where the phase is locked, (6) becomes

$$I_s\cdot\sin(\varphi_0-\psi_0) = 2\cdot C\cdot\hat{V}_l\cdot\Delta\omega_0 \tag{7}$$

and (5) becomes

$$\left(\frac{\omega_0}{Q_0} + \frac{1}{C}\cdot\left(b + \frac{3}{4}\cdot d\cdot\hat{V}_l^2\right)\right) = \frac{I_s}{\hat{V}_l}\cdot\frac{\omega}{C}\cdot\cos(\psi_0-\varphi_0). \tag{8}$$

The steady state of this synchronized regime, defined by $\hat{V}_l(t) = V_0$, $\varphi(t) = \varphi_0$, $\psi(t) = \psi_0$, and $\Delta\omega = \Delta\omega_0$ is perturbated in two different ways. First, there exists an external perturbation of the ψ_0 phase of the synchronizing oscillator named $\delta\psi(t)$. Firstly, note that the amplitude perturbation of this synchronizing source is supposedly negligible. Secondly, the oscillator is perturbated by an internal noise source, which can be represented by an equivalent frequency deviation $\delta\omega(t)$. The phase $\varphi(t)$ and amplitude $\hat{V}_l(t)$ of the synchronized oscillator become, respectively, $\varphi_0 + \delta\varphi(t)$ and $V_0 + \delta V(t)$. By taking into account these perturbations and (7) and (8), Adler's equation can be written as

$$\frac{\delta V}{V_0} = \frac{\delta\varphi - \delta\psi}{tg(\psi_0-\varphi_0)} + \frac{\left(\dfrac{d\delta\varphi}{dt} - \delta\omega\right)}{\Delta\omega_0}. \tag{9}$$

In the same way, the perturbation of (6) with the assumption $d\delta\varphi/dt \ll \omega$ gives

$$\begin{aligned}&\frac{d^2\delta\varphi}{dt^2}\cdot V_0 + 2\cdot\omega\cdot\frac{d\delta V}{dt} + \frac{\delta V}{V_0}\cdot\omega\\ &\quad\cdot\left(\frac{\omega_0}{Q_0} + \frac{1}{C}\left(b + \frac{9}{4}\cdot d\cdot V_0^2\right)\right)\cdot V_0\\ &\quad = -\frac{I_s\cdot\omega}{C}\cdot\sin(\psi_0-\varphi_0)\cdot(\delta\psi-\delta\varphi).\end{aligned} \tag{10}$$

Using (9) and its time derivative with the assumption that $\Delta\omega_0 \ll 2\cdot\omega$, (10) may be written as

$$\begin{aligned}&\frac{2}{\alpha}\frac{d^2\delta\varphi}{dt^2} + \left(\frac{2\cdot\Delta\omega_0}{\alpha\cdot tg(\psi_0-\varphi_0)} + 1\right)\frac{d\delta\varphi}{dt}\\ &\quad + \left(\frac{I_s\cdot\Delta\omega_0}{\alpha\cdot V_0\cdot C}\sin(\varphi_0-\psi_0) + \frac{\Delta\omega_0}{tg(\varphi_0-\psi_0)}\right)\delta\varphi\\ &= \frac{2\cdot\Delta\omega_0}{\alpha\cdot tg(\psi_0-\varphi_0)}\frac{d\delta\psi}{dt}\\ &\quad + \left(\frac{I_s\cdot\Delta\omega_0}{\alpha\cdot V_0\cdot C}\sin(\varphi_0-\psi_0) + \frac{\Delta\omega_0}{tg(\varphi_0-\psi_0)}\right)\delta\psi\\ &\quad + \frac{2}{\alpha}\cdot\frac{d\delta\omega}{dt} + \delta\omega\end{aligned} \tag{11}$$

where $\alpha = \omega_0/Q_0 + 1/C\cdot(b + \frac{9}{4}\cdot d\cdot V_0^2)$.

This equation represents the dynamic behavior of the circuit. If there exists a phase modulation $\delta\psi$ of the synchronizing oscillator, by resolving (10) it is possible to express the output phase modulation $\delta\varphi$. Equation (11) appears to be a linear second-order differential equation, which is analogous to the dynamic equation of an analog PLL, shown in Fig. 2. This equation relates the output phase $\delta\varphi$ to the input phase $\delta\psi$ and the internal perturbation $\delta\omega$ as follows [5]:

$$\begin{aligned}&\tau_1\cdot\frac{d^2\delta\varphi}{dt^2} + (1 + K\cdot\tau_2)\cdot\frac{d\delta\varphi}{dt} + K\cdot\delta\varphi\\ &\qquad = K\cdot\tau_2\cdot\frac{d\delta\psi}{dt} + K\cdot\delta\psi + \tau_1\cdot\frac{d\delta\omega}{dt} + \delta\omega\end{aligned} \tag{12}$$

where K is the open-loop gain of the PLL, and τ_1 and τ_2 are the two time constants of the phase–lag filter of the loop, which has a transfer function that reads as

$$F(j\cdot\Omega) = \frac{1 + j\cdot\Omega\cdot\tau_2}{1 + j\cdot\Omega\cdot\tau_1}, \qquad \text{with } \tau_1 > \tau_2. \tag{13}$$

By comparing (11) and (12), the parameters $(K,\ \tau_1,\ \tau_2)$ of the PLL can be related to those of the Van Der Pol synchronized oscillator by

$$\begin{aligned}\tau_1 &= \frac{2}{\alpha}\\ K &= \frac{I_s\cdot\Delta\omega_0\cdot\sin(\varphi_0-\psi_0)}{\alpha\cdot V_0\cdot C} + \frac{\Delta\omega_0}{tg(\varphi_0-\psi_0)}\\ \tau_2 &= \frac{2\cdot\Delta\omega_0}{\alpha\cdot tg(\psi_0-\varphi_0)\cdot K}.\end{aligned} \tag{14}$$

Resolving (12) in the frequency domain, it is then possible to express the output phase-noise spectral density $S_\Phi(\Omega) = \langle|\delta\varphi|^2\rangle$ as a

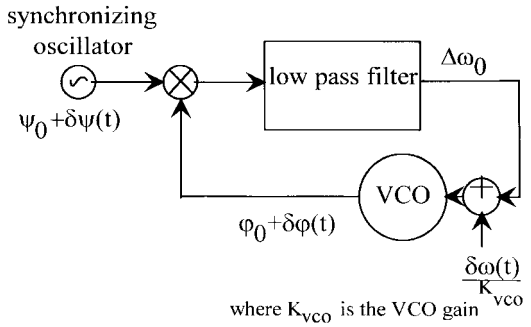

Fig. 2. Block diagram of an equivalent PLL.

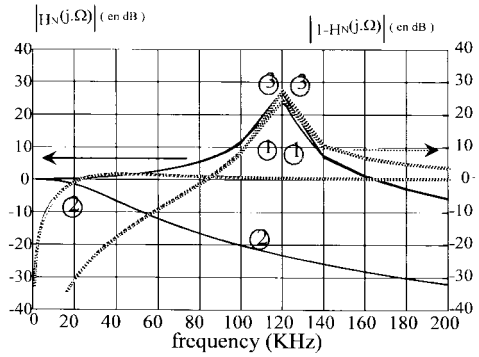

Fig. 3. $|H_N(j \cdot \Omega)|$ and $|1 - H_N(j \cdot \Omega)|$ versus offset frequency.

function of the input phase-noise spectral density of the synchronizing oscillator $S_\Psi(\Omega) = \langle|\delta\psi|^2\rangle$ and the internal phase-noise spectral density, which represents the phase-noise spectral density of the free-running oscillator $S_{\Theta_i}(\Omega) = \langle|\delta\omega|^2\rangle/4 \cdot \pi^2 \cdot \Omega^2 \cdot K_{\text{vco}}^2$, with the following relation:

$$S_\Phi(\Omega) = |H(j \cdot \Omega)|^2 \cdot S_\Psi(\Omega) + |1 - H(j \cdot \Omega)|^2 \cdot S_{\Theta_i}(\Omega) \quad (15)$$

where $H(j \cdot \Omega) = [K \cdot F(j \cdot \Omega)]/[j \cdot \Omega + K \cdot F(j \cdot \Omega)]$ is the system transfer function of the PLL [6]. It should be noted that the parameters of (12), namely K, τ_1, and τ_2, depend in a nonlinear fashion on the oscillator parameters and detuning frequency $\Delta\omega = \omega_0 - \omega$. Thus, it will be necessary to calculate these parameters for each steady state in the locking bandwith. The magnitude of the system transfer function $H(j \cdot \Omega)$ can be expressed in the normalized form

$$|H_N(\omega_n)|^2 = \frac{1 + \left(2 \cdot \xi - \frac{\omega_0}{K}\right)^2 \cdot \omega_n^2}{(1 - \omega_n^2)^2 + 4 \cdot \xi^2 \cdot \omega_n^2},$$

$$\text{with normalized pulsation } \omega_n = \frac{\Omega}{\omega_0} \quad (16)$$

where ξ is the damping factor. The expression of ω_0 and ξ of the PLL are given by

$$\omega_0^2 = \frac{K}{\tau_1}$$
$$2 \cdot \xi \cdot \omega_0 = \frac{1 + K \cdot \tau_2}{\tau_1}. \quad (17)$$

The nonlinear steady-state analysis of the synchronized oscillator is carried out by means of a modified harmonic-balance software [7] and has permitted the determination of the frequency-locking range between 2.495 875–2.496 15 GHz and the oscillator parameters $\Delta\omega_0$, φ_0, V_0. Using (14) and (17), the damping factor and natural frequency $f_0 = \omega_0/2\pi$ can be calculated. The magnitudes of the system transfer function $|H_N(j \cdot \Omega)|$ and the voltage-controlled

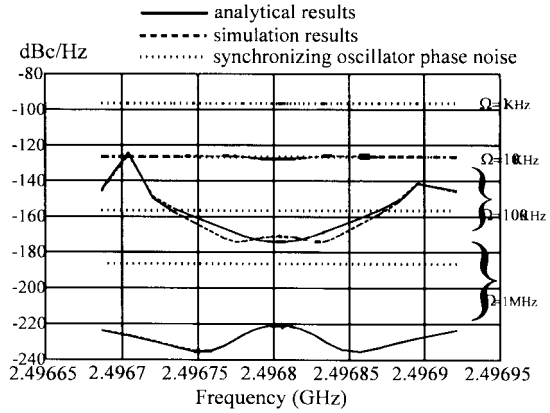

Fig. 4. Comparison between simulated and calculated output phase-noise spectrum of the synchronized oscillator versus locking bandwidth for the four frequencies offset from carrier 1, 10, and 100 kHz, and 1 MHz.

oscillator (VCO) phase error transfer function $|1 - H_N(j \cdot \Omega)|$ [6] are plotted in Fig. 3, as a function of the distance from the carrier for different values of the damping factor and natural frequency. As expected, these transfer functions correspond to a low- and high-pass filter, respectively, and the curves have a peak at $\Omega = \omega_0$; the amplitude increases with decreasing ξ. With the help of (15), one can deduce the contributions to the output phase-noise spectrum from the intrinsic and injected noise. This shows that the near-carrier phase-noise spectrum is mainly due to the injected noise by the contribution of the equivalent low-pass filter $|H_N(j \cdot \Omega)|$ and the far-carrier phase-noise spectrum is mainly due to the intrinsic noise by the contribution of the equivalent high-pass filter $|1 - H_N(j \cdot \Omega)|$. The rigorous nonlinear noise analysis [4] can be used to calculate the output noise spectrum for the whole locking range. Fig. 4 shows the output phase-noise spectrum obtained, by the application of the PLL formula (15) and by means of the nonlinear simulator, as a function of the locking band for the four offset frequencies 1 kHz, 10 kHz, 100 kHz, and 1 MHz. We note very good agreement between the simulated and analytical results.

III. Conclusion

This paper discusses in detail an original approach to predict the noise behavior of a synchronized oscillator based on PLL theory. Based on the works of Adler, we have established a perturbation equation, which permitted us to carry out an analytical expression of a phase-noise spectrum of a free and synchronized oscillator. It provides a good understanding and mathematical explanations of the noise behavior in the whole locking bandwidth. This circuit has permitted us to validate our simulator based on frequency-conversion formalism. This circuit could serve as a benchmark in testing commercial nonlinear noise simulators to evaluate their capabilities.

References

[1] K. F. Schunemann and K. Behm, "Nonlinear noise theory for synchronized oscillators," *IEEE Trans. Microwave Theory Tech.*, vol. MTT-27, pp. 452–458, May 1979.

[2] M. T. Vlaardingerbroek and J. J. Goedbloed, "In the theory of noise and injection phase locking of IMPATT diode oscillators," *Philips J. Res.*, vol. 25, pp. 452–471, Dec. 1970.

[3] X. Zhang, X. Zhou, and A. S. Daryoush, "A theoretical and experimental study of the noise behavior of subharmonically injection locked local oscillators," *IEEE Trans. Microwave Theory Tech.*, vol. 40, pp. 895–902, May 1992.

[4] J. M. Paillot, J. C. Nallatamby, M. Hessane, R. Quere, M. Prigent, and J. Rousset, "A general program for steady state and FM noise analysis of microwave oscillators," in *IEEE MTT-S Int. Microwave Symp. Dig.*, Dallas, TX, 1990, pp. 287–1290.
[5] R. Adler, "A study of locking phenomena in oscillators," *Proc. IRE*, vol. 34, pp. 351–357, June 1946.
[6] A. Blanchard, *Technique des boucles d'asservissement de phase*. Paris, France: Cours de l'École Supérieure d'Électricité, Univ. Paris, 1975.

Static Analysis of Arbitrarily Shaped Conducting and Dielectric Structures

Sadasiva M. Rao and Tapan K. Sarkar

***Abstract*— In this paper, a simple and efficient numerical procedure is presented to compute the charge distribution and capacitance of conducting bodies in the presence of dielectric structures of arbitrary shape and finite size. The method presented is robust and provides accurate results for both low as well as high dielectric-constant materials as supported by numerical examples.**

***Index Terms*—Capacitance, dielectric bodies, electrostatic analysis, moment methods.**

I. Introduction

In [1], Rao *et al.* described the evaluation of static charge distribution and capacitance matrices for conductors of finite size in the presence of dielectric media. Recently, this formulation was also incorporated into a fast multipole method to generate a computationally fast algorithm [2], [3]. Although the work presented in [1] and [2] is general, it is computationally expensive. In [1], the total charge is computed everywhere by solving a set of integral equations, the free charge on conductors is then obtained by solving yet another integral equation. Thus, the free-charge extraction is a two-step procedure and, computationally, this implies storing and inverting large matrices. Further, the method presented in [1] may be inaccurate, as shown in [3], for the case of high-dielectric materials.

In this paper, we present a simple and efficient procedure to obtain the free charge on the conductors in the presence of dielectric materials which may have low as well as large ϵ_r. The main advantage of this technique is the elimination of the expensive two-step procedure and calculating the free charge in a straightforward manner.

II. Integral-Equation Formulation

Consider a system of finite length, and finite- or zero-thickness conductors situated in the presence of dielectric bodies, as shown in Fig. 1. Let N_c and N_d represent the total number of disjoint conductors and dielectric bodies, respectively, which are present in the system configuration. The whole system is immersed in free space and could be placed on a ground plane of either finite or infinite size.

Manuscript received April 24, 1997; revised May 11, 1998.

S. M. Rao is with the Department of Electrical Engineering, Auburn University, Auburn, AL 36849 USA.
T. K. Sarkar is with the Department of Electrical Engineering and Computer Science, Syracuse University, Syracuse, NY 13244 USA.

Publisher Item Identifier S 0018-9480(98)05500-8.

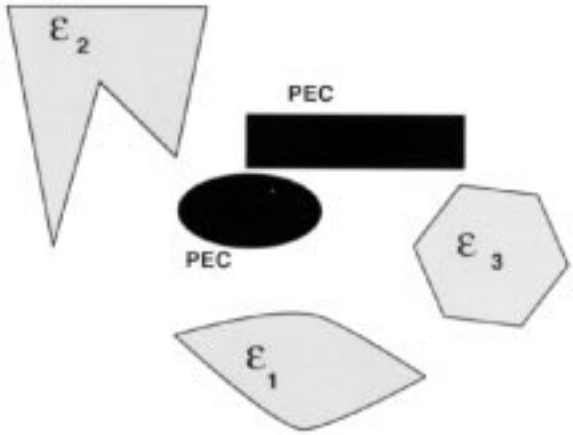

Fig. 1. Conducting and dielectric structures in the homogeneous medium.

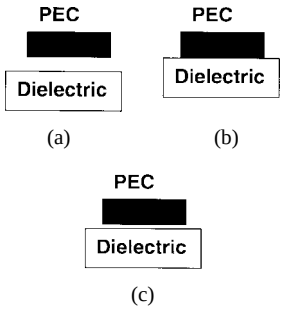

Fig. 2. Numerical modeling procedure.

In this formulation, the central idea is that we treat each conductor and each dielectric body as if it is immersed in free space. Thus, we consider a combination of the conductor–dielectric interface as two bodies separated by zero distance. In this way, we treat all dielectric bodies as closed surfaces. If the conducting and dielectric bodies are separated by a finite distance, as shown in Fig. 2(a), the treatment is obvious. However, if the conductor and dielectric bodies are joined together, as shown in Fig. 2(b), we treat them as two bodies with a layer of zero-thickness free space separating them, as shown in Fig. 2(c).

In applying the equivalent charge formulation, we first replace each conducting and dielectric surface by surface charges σ_c and σ_d, respectively. Using the mathematical procedures described in [1], we derive a set of integral equations, given by

$$\sum_{i=1}^{N_c+N_d} \frac{1}{4\pi\epsilon_0} \int_{S_i} \frac{\sigma(\boldsymbol{r}')}{|\boldsymbol{r}-\boldsymbol{r}'|}\, ds' = V_j(\boldsymbol{r}), \qquad \boldsymbol{r} \in S_j,\ j = 1, 2, \cdots, N_c \quad (1)$$

and

$$2\pi(1+\epsilon_{rj})\sigma(\boldsymbol{r})+(1-\epsilon_{rj}) \sum_{i=1}^{N_c+N_d} \int_{S_i} \frac{\sigma(\boldsymbol{r}')(\boldsymbol{r}-\boldsymbol{r}')\cdot \boldsymbol{a}_{nj}}{|\boldsymbol{r}-\boldsymbol{r}'|^3}\, ds' = 0, \qquad \boldsymbol{r} \in S_j,\ j = N_c+1, N_c+2, \cdots, N_c+N_d \quad (2)$$

where V_j is the potential on the jth conductor, ϵ_{rj} and $\boldsymbol{a}_{nj}$ are the dielectric constant and unit outward normal of the jth dielectric body, and σ is the unknown charge density equal to σ_c or σ_d. Note that $\boldsymbol{a}_{nj}$ may be uniquely defined since the dielectric body is a closed body.